Finite-temperature dynamics of the Mott insulating Hubbard chain

Alberto Nocera,[1,2] Fabian H. L. Essler,[3] and Adrian E. Feiguin[4]
[1]*Department of Physics and Astronomy, University of Tennessee, Knoxville, Tennessee 37966, USA*
[2]*Materials Science and Technology Division, Oak Ridge National Laboratory, Oak Ridge, Tennessee 37831, USA*
[3]*Rudolf Peierls Centre for Theoretical Physics, University of Oxford, Oxford OX1 3NP, United Kingdom*
[4]*Department of Physics, Northeastern University, Boston, Massachusetts 02115, USA*

(Received 16 October 2017; published 29 January 2018)

We study the dynamical response of the half-filled one-dimensional Hubbard model for a range of interaction strengths U and temperatures T by a combination of numerical and analytical techniques. Using time-dependent density matrix renormalization group computations we find that the single-particle spectral function undergoes a crossover to a spin-incoherent Luttinger liquid regime at temperatures $T \sim J = 4t^2/U$ for sufficiently large $U > 4t$. At smaller values of U and elevated temperatures the spectral function is found to exhibit two thermally broadened bands of excitations, reminiscent of what is found in the Hubbard-I approximation. The dynamical density-density response function is shown to exhibit a finite-temperature resonance at low frequencies inside the Mott gap, with a physical origin similar to the Villain mode in gapped quantum spin chains. We complement our numerical computations by developing an analytic strong-coupling approach to the low-temperature dynamics in the spin-incoherent regime.

DOI: 10.1103/PhysRevB.97.045146

I. INTRODUCTION

The physics of one-dimensional metals can generally be described in terms of Luttinger liquid theory. In a Luttinger liquid (LL) [1–3], the natural excitations are collective density fluctuations, that carry either spin ("spinons"), or charge ("holons"). This leads to the spin-charge separation picture, in which a fermion injected into the system breaks down into excitations carrying different quantum numbers, each with a characteristic energy scale and velocity (one for the charge, one for the spin). A key paradigm for this kind of behavior is provided by the one-dimensional Hubbard model:

$$H = -t \sum_{i=1,\sigma}^{L} (c^{\dagger}_{i\sigma} c_{i+1\sigma} + \text{H.c.}) + U \sum_{i=1}^{L} \left(n_{i\uparrow} - \frac{1}{2}\right)\left(n_{i\downarrow} - \frac{1}{2}\right). \quad (1)$$

Here, $c^{\dagger}_{i\sigma}$ creates an electron of spin σ on the ith site along a chain of length L. The Coulomb repulsion is parametrized by U, and we take the interatomic distance as unity. We express all energies in units of the hopping parameter t.

A remarkable aspect of this model is that it is integrable: it contains an extensive number of local integrals of motion that allow one to exactly solve it with the Bethe ansatz [4]. Whereas the low-energy physics of the one-dimensional (1d) Hubbard model below half filling is described in terms of LL theory [5], at half filling (density of particles $n = 1$, or number of particles $N = L$) the model has a Mott insulating ground state, with a charge gap that grows exponentially with U for weak interactions. The spin excitations, however, remain gapless and the system exhibits algebraically decaying antiferromagnetic spin-spin correlations. Mott insulators defy conventional paradigms, since the rigid band picture underlying the physics of semiconductors does not apply [6,7]: in strongly interacting systems, the "bands" change with doping, giving rise to a complex phenomenology that includes hole pockets, Fermi arcs, and kinks [8,9].

The zero-temperature dynamical properties of the Hubbard model have been studied in great detail by a variety of analytic and numerical methods both in the metallic [5,10–29] and the Mott insulating [30–34] phases. The finite-temperature dynamics is less well understood. The single-particle spectral function below half filling has been previously studied by quantum Monte Carlo [35] and density matrix renormalization group (DMRG) [36] methods. The half-filled case was considered in Ref. [37] in the small to intermediate temperature regime, $T \leqslant t$, using the quantum Monte Carlo (QMC) method with maximum-entropy analytic continuation procedures. The low-temperature regime for small Mott gaps $T \lesssim \Delta \ll t$ was analyzed by field theory methods in Ref. [38]. As a result of spin-charge separation one-dimensional metals and Mott insulators can display very unusual behavior at finite temperatures. An example is the so-called "spin-incoherent" Luttinger liquid regime [39–45], which occurs in the metallic case if the spinon bandwidth is much smaller than the holon bandwidth, which corresponds to $U \gg t$ in the case of the Hubbard chain. In this regime a small temperature makes the spin degrees of freedom completely incoherent, while the charge degrees of freedom remain close to the ground state. In this situation, excitations effectively behave as "spinless fermions" and this has dramatic effects on the spectral functions [46,47].

The finite-temperature dynamics of quasi-one-dimensional Mott insulators has been investigated in a number of cases. Spin-charge separation was observed in photoemission experiments on the chain cuprates $SrCuO_2$ [48–50] and Sr_2CuO_3 [51]. In these materials the characteristic energy scales for

spin and charge degrees of freedom are very large, so that the achievable temperatures are always small compared to the Mott gap. The experimental findings could not be accounted for by a simple t-J model at zero temperature. ARPES measurements on the one-dimensional Mott insulator $Na_{0.96}V_2O_5$ show that the spectral density of the lower Hubbard band is strongly dependent on the temperature [52]. Simple broadening and charging effects could not explain the dramatic spectral weight redistribution as a function of temperature, which was attributed to strong correlation effects in the material. Exact diagonalization studies of a t-J model presented discrepancies with the experimental results. In particular, while theory and experiment agreed well for small momentum transfers and at low energy, a long tail of excitations at high energies for intermediate to large momentum transfers (up to the Brillouin zone boundary) was observed and not accounted for by the theory. Some of the experimentally observed effects are expected to be due to the fact that the appropriate effective Hamiltonians for the various materials will contain longer-range hoppings and interactions, while others will be due to finite temperatures. To get a qualitative understanding of the latter it is clearly useful to investigate the dynamics of the one-dimensional Hubbard model in a range of temperatures.

Experimentally probing the high-temperature dynamics at a fixed density has remained a challenge, since the Mott gap is on the order of or higher than the melting point of some materials. However, several ongoing efforts in the cold-atom community are focused on studying the excitations of spinful fermionic systems [53], particularly in one dimension [54].

The paper is structured as follows: In Sec. II we briefly describe the computational methods; in Sec. III we present the results of our finite-temperature simulations. Section IV describes an analytical approach for the spin-incoherent regime. We close with a summary and discussion.

II. NUMERICAL APPROACH

In this work we would like to explore the entire temperature regime at half filling. For this purpose we resort to finite-temperature time-dependent DMRG calculations (tDMRG) [55–58]. Even though the method has been extensively discussed in the literature [59], particularly in a recent review [58], we proceed to describe it in a condensed form.

The calculation relies on ideas from thermofield dynamics [60–66]. This construction allows one to represent a mixed state of a quantum system as a pure state in an enlarged Hilbert space. Consider the energy eigenstates of the system in question $\{n\}$, described by a Hamiltonian H, and introduce an auxiliary set of fictitious states $\{\tilde{n}\}$ in one-to-one correspondence with $\{n\}$. We can then define the unnormalized pure quantum state,

$$|\psi(\beta)\rangle = e^{-\beta H/2}|\psi(0)\rangle = \sum_n e^{-\beta E_n/2}|n\tilde{n}\rangle, \tag{2}$$

where $\tilde{n}$ is a copy of n in the auxiliary Hilbert space, $\beta = 1/T$ is the inverse temperature, and $|\psi(0)\rangle = \sum_n |n\tilde{n}\rangle$ is our thermal vacuum. Then the exact thermodynamic average of an operator $\hat{O}$ (acting only on the real states) is given by

$$\langle\hat{O}\rangle = Z(\beta)^{-1}\langle\psi(\beta)|\hat{O}|\psi(\beta)\rangle. \tag{3}$$

Here, the partition function is the norm of the thermal state $Z(\beta) = \langle\psi(\beta)|\psi(\beta)\rangle$. Hence, a thermodynamic average reduces to a conventional expectation value in a pure quantum state.

At $\beta = 0$, the state $|\psi(0)\rangle$ is the maximally entangled state between the real system and the fictitious system. We can see that this is independent of the representation, and we can choose any arbitrary basis.

The most technical aspect concerns the choice of initial state at $\beta = 0$. One can pick to work in either the grand canonical or the canonical ensemble [36,67,68], and this will determine the method to initialize the simulations. In order to work in the canonical ensemble we need to start from a thermal vacuum where the physical states $|n\rangle$ and their copies $|\tilde{n}\rangle$ have each a fixed number of particles. This requires one to construct a state that is a sum of all possible states of charge and spin, with the constraint that the total number of particles on the chain has to be equal to N, and that the charge state of the ancillas is an exact copy of the charge state of the physical chain. In order to generate this state, we use the conventional ground-state DMRG algorithm with a very peculiar Hamiltonian (we can call it the "entangler Hamiltonian"):

$$H_{\text{ent}} = -\sum_{i\neq j\,\sigma}(\Delta^\dagger_{i\sigma}\Delta_{j\sigma} + \text{H.c.}). \tag{4}$$

The operator $\Delta^\dagger(\Delta)$ is given by

$$\Delta^\dagger_{i\sigma} = c^\dagger_{i\sigma}\tilde{c}^\dagger_{i\sigma}, \tag{5}$$

where the "tilde" operators act on the ancillas on site i. The ground state of this Hamiltonian is precisely the equal superposition of all possible configurations of N "physical site-ancilla" pairs on L sites.

The Green's function at time t and inverse temperature β is obtained as

$$G(x - x_0, t, \beta) = \langle\psi(\beta)|e^{i\hat{H}t}\hat{O}^\dagger(x)e^{-i\hat{H}t}\hat{O}(x_0)|\psi(\beta)\rangle, \tag{6}$$

where the generic operators of interest $\hat{O}(x)$, $\hat{O}^\dagger(x)$ act on the system at site x. The time evolution is dictated by the Hamiltonian $\hat{H} = H - \tilde{H}$; H governs the physics of the actual physical chain, not including the ancillas, while $\tilde{H}$ is an exact copy of H acting on the ancillas [69].

The calculation proceeds as follows: First, we evolve the maximally entangled state in imaginary time to the desired value of β (measured in units of the hopping t). Then, an operator $\hat{O}(x_0 = L/2)$ is applied in the center of the chain. The resulting state is evolved in real time, and at every step we measure the overlap with the state $\hat{O}(x)e^{-i(H-\tilde{H})t}|\psi(\beta)\rangle$. We obtain the desired Green's function in frequency and momentum by Fourier-transforming the results in real space and time. In this work we use a third-order Suzuki-Trotter decomposition with a typical time step $\tau_\beta = 0.05$ and $\tau = 0.05$ for the real-time and imaginary-time parts of the simulation, and keeping 800 DMRG states, enough to maintain the truncation error below 10^{-5}. The chain length is fixed to $L = 40$ sites, and the real-time window has a range $t_{\max} = 15$.

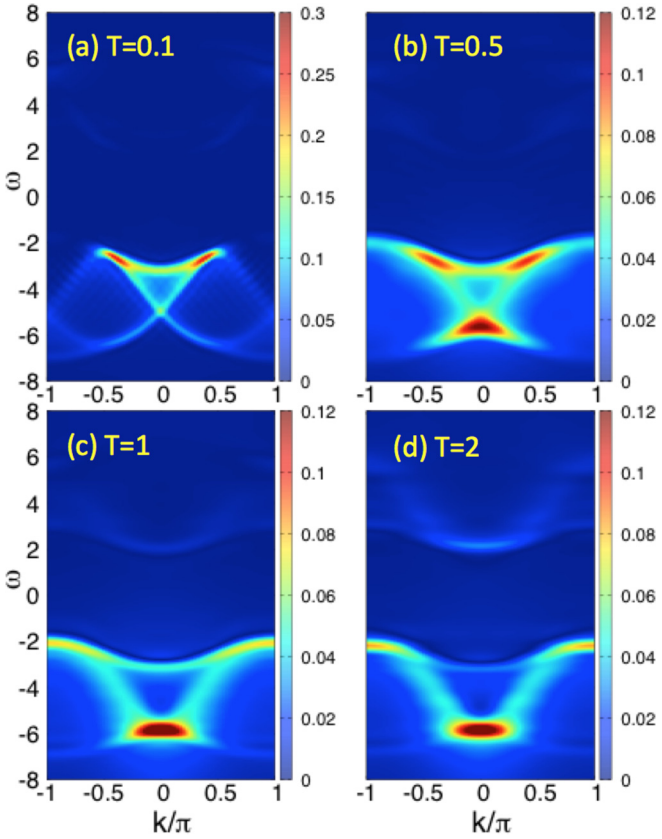

FIG. 1. Photoemission spectrum for the 1d Hubbard model with $U/t = 8$ calculated with tDMRG at four different temperatures.

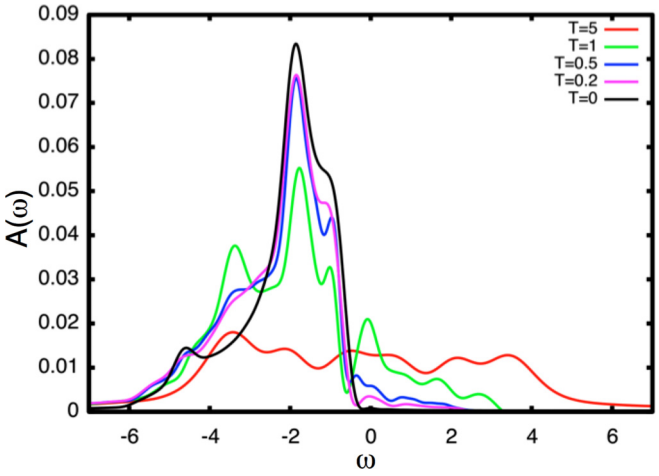

FIG. 2. Integrated photoemission spectrum (occupied fraction of the total density of states) for the 1d Hubbard model at half filling with $U/t = 4$ obtained with tDMRG at different temperatures.

III. RESULTS

A. Single-particle spectral function

The electronic spectrum of the Hubbard model can be qualitatively understood in the $U \to \infty$ limit [70,71], where spin-charge separation is exact. In this regime, all eigenstates factorize into a product of a fermionic wave function and a spin wave function. This leads to a simple and elegant description [72,73]: assuming that the dispersion of holons is given by $\epsilon_h(q_h) = -2t \cos q_h$, and the one for spinons by $\epsilon_s(q_s) = J \cos q_h$, with $J = 4t^2/U$, one can construct all possible energies with momentum k as $\epsilon(k) = \epsilon_h(q_h) + \epsilon_s(q_s)$, with $k = q_h + q_s$. Clearly, this construction will yield a continuum of energies with momentum k: the Fermi liquid description breaks down, and there is no fermionic quasiparticle in the Landau sense. The elementary excitations of the Hubbard model can then be summarized as spinons, and holons below the Fermi energy. Holons are defined between $q_h = \pm 2k_F$, and removing a particle from the system corresponds to creating deconfined spinon-holon pairs. The excitations for adding a particle lead to the creation of spinon-antiholon pairs above the Fermi energy. Antiholons are defined in the intervals $[-\pi, -2k_F]$ and $[2k_F, \pi]$ and usually refer to *empty* states as shown in Fig. 3(a). Notice that this picture also applies to the upper Hubbard band, but in this case we name the particle excitations "doublons."

In Fig. 1 we show the photoemission part of the spectral function for $U/t = 8$ and four different temperatures, obtained with a choice of operators $\hat{O} = c$ (the annihilation operator); this corresponds to the *occupied* electronic states. At low temperatures (upper panels) we can clearly resolve both holon and spinon bands. Even at small temperatures relative to the gap, we see that there is a finite occupation of the upper Hubbard band. Most remarkably, for increasing temperatures, we find spectral weight leaking into the gap. As doublons are created, holes are left behind in the lower Hubbard band and thermally excited quasiparticles can now occupy these states. This gives rise to weight in the gap due to anomalous spectral transfer [6]. Near the Fermi level, high-energy electrons can now occupy states that are attributed to antiholons, which at zero temperature are always *empty* states. The antiholon-spinon continuum leaks into the gap near the Mott transition [74], as we see in Fig. 3. The thermal excitations can be traced back to the antiholon-spinon continuum that appears in the gap, and their particle-hole conjugates in the upper Hubbard band. This leads to a melting of the gap which is even more dramatic at smaller values of U/t, as seen in Fig. 2 where we display the photoemission spectrum integrated over momentum: for $U/t = 4$ the gap is gone altogether at small temperatures. In addition, while the Mott gap is melting, spectral weight is redistributed to large and negative energies, in qualitative agreement with the experimental results in Ref. [52]. The origin of the in-gap states can be traced back to the zero-temperature spectra of the doped Mott insulator. For illustration, in Fig. 3 we show the zero-temperature spectrum of the chain with 2 holes and 2 electrons. The states below (above) the Fermi level are occupied (empty) and the spinon-antiholon branches are responsible for the leakage of spectral weight into the gap. We clearly see that the mere addition/subtraction of a particle can completely melt the Mott gap *in the finite system* considered. In the thermodynamic limit, a finite density of holes would be required to make this effect observable. However, a finite temperature induces similar effects. An important issue to address is the behavior of the spin excitations with temperature [35]. As we see in our results for $U/t = 8$, the "two-branch" spectrum characteristic of a Luttinger liquid survives to temperatures on the order of $T \sim J$. That is when the crossover to the spin-incoherent regime takes place: at higher

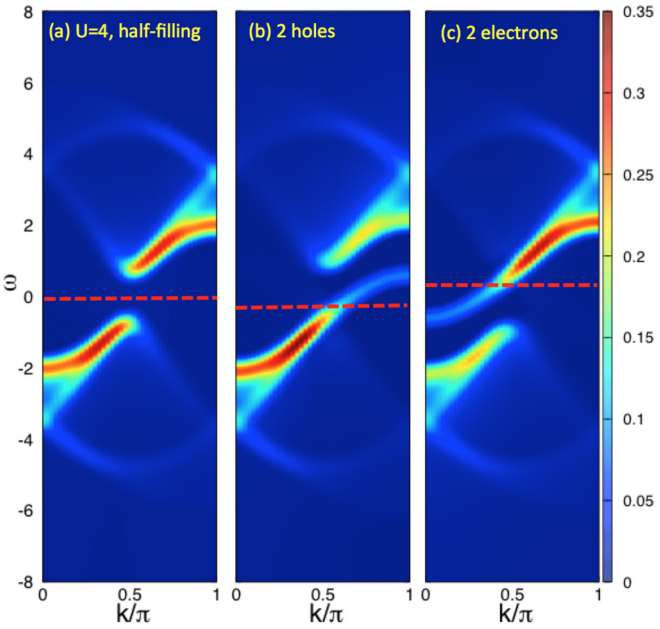

FIG. 3. Zero-temperature spectral function of the 1d Hubbard model with $U/t = 4$ calculated with tDMRG at three different densities: (a) half filling, (b) 2-hole doping, and (c) 2 additional electrons. The dashed line indicates the position of the chemical potential. The mere addition/subtraction of a single particle immediately destroys the Mott gap.

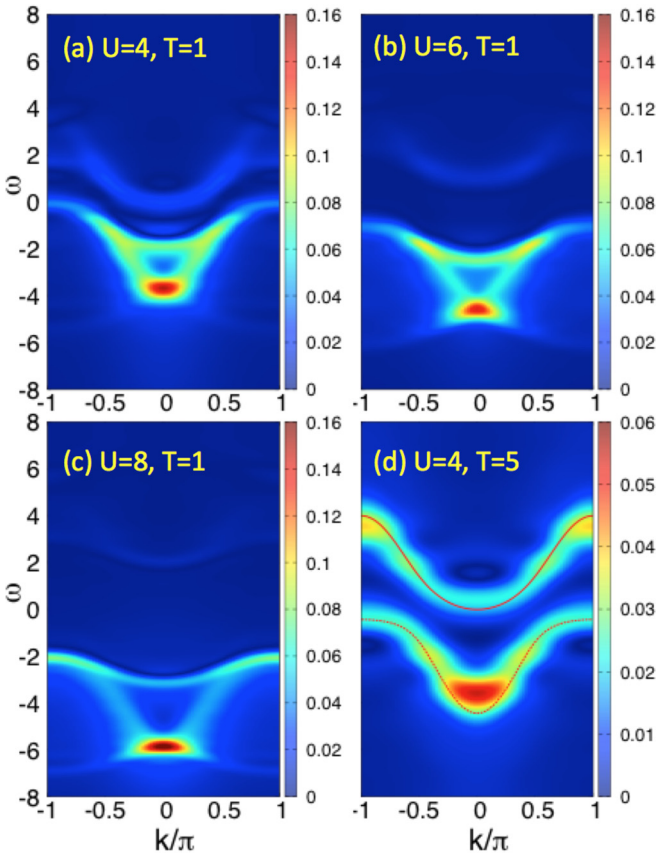

FIG. 4. (a)–(c) Photoemission spectrum for the 1d Hubbard model with $U/t = 4,6,8$ and $T = 1$ calculated with tDMRG. In panel (d) we show results for $U = 4$ and $T = 5$. We have included the dispersion obtained from the Hubbard-I approximation (see text), with a renormalized U_{eff}.

temperatures the spinons are effectively thermalized, and the spectrum resembles that of spinless fermions with a single branch $\epsilon(k) = -2t\cos(k)$. This is remarkable considering that the excitations are completely determined by the Hamiltonian, and do not change with temperature: what changes is the distribution of spectral weight. We need to recall that the electronic Green's function is a convolution of the charge and spin Green's functions. At large values of U the spinon band is less dispersive than the charge excitations and the spectral weights will respond differently for each kind of excitation. The charge will behave as though in the ground state, but the redistribution of spectral weight in the spin Green's function will lead to a bandlike feature that shifts *in momentum*. We refer the reader to Refs. [46,47] for a detailed description of the phenomenon. Notice that our results are in qualitative agreement with those obtained in Ref. [37], where the authors used QMC with maximum-entropy analytic continuation procedures in the low-temperature regime.

For smaller values of U/t we do not find spin-incoherent behavior. In this case the spin and charge dispersions have broad bandwidths, and all degrees of freedom will get similarly excited. At temperatures larger than the hopping $T > t$, we find completely incoherent upper and lower Hubbard bands. This regime can be qualitatively described in terms of a Hubbard-I mean-field approximation [75,76], with interacting doublon and holon excitations that ignore the magnetic correlations. In this case the two bands are given by

$$E_{\pm}(k) = \epsilon(k) \pm \sqrt{\epsilon(k)^2 + \left(\frac{U_{\text{eff}}}{2}\right)^2}, \tag{7}$$

where $\epsilon(k) = -2t_{\text{eff}}\cos(k)$ is once again the noninteracting dispersion but with a renormalized hopping. In the original formulation, the excitations are expected to be twice as heavy ($t_{\text{eff}} = t/2$) because, due to the spin-incoherent background, a hole or doublon has half the probability to hop to a neighboring site. This approach works very well in 2d at high temperatures, but as we see in Fig. 4(d), in one dimension the bandwidth remains unaffected, with $t_{\text{eff}} = t$ and an effective $U_{\text{eff}} \leqslant U$. This is attributed once again to spin-charge separation: in one dimension the holon and doublon excitations can be assumed to be spinless quasiparticles with hopping t, regardless of the spin background.

B. Villain-like mode

An interesting feature in the dynamical response of gapped many-particle systems is finite-temperature resonances at low frequencies. The paradigm for this kind of behavior is the so-called Villain mode [77] in the spin-1/2 Heisenberg chain. The mechanism underlying this feature is straightforward: at temperatures of the order of the gap, a thermal population of spin excitations will result in a dynamical spin response at low energies $\omega \sim 0$ due to transitions between thermally occupied states. The weight of these contributions to the dynamical spin structure factor increases with temperature at low $T < \Delta$,

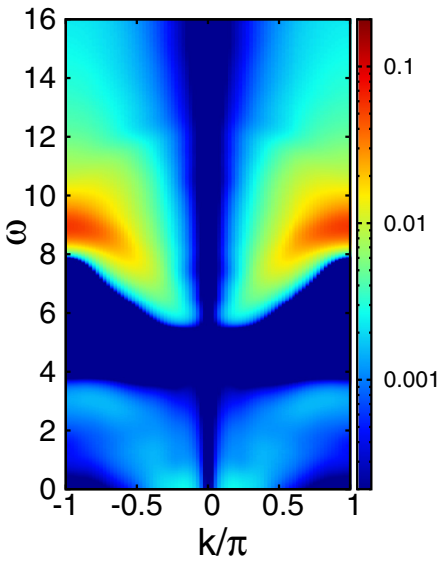

FIG. 5. Charge dynamical structure factor for $U = 8, T = 1$. The finite spectral weight at low frequencies is a result of intraband transitions. Notice that color density is in a logarithmic scale.

where Δ is the $T = 0$ gap. Interestingly, the spectral weight is strongly concentrated around some "dispersion" $E(Q)$ [77–79].

The charge excitations in the $U > 0$ Hubbard chain are in one-to-one correspondence with the spin excitations of its $U < 0$ counterpart via a particle-hole transformation, such that the Mott charge gap translates into a spin gap. Therefore, one may expect a Villain-like mode to emerge in the dynamical *density-density* correlation function in the repulsive case. Figure 5 illustrates this for $U = 8$ and $T = 1$, where we plot results for the operator $\hat{O}(x) = n(x) - 1$ ($n = n_\uparrow + n_\downarrow$ is the density operator). The offset allows us to resolve the density fluctuations and eliminates large contributions at $k = 0$ [67]. The low-energy features can be understood in the framework of the analytical strong-coupling approach developed in Sec. IV.

IV. ANALYTIC APPROACH TO THE SPIN-INCOHERENT REGIME AT LARGE U

In this section we develop an analytic approach to the dynamics in the spin-incoherent regime in the $U \to \infty$ limit of the Hubbard model. Our starting point is the Hamiltonian for the repulsive half-filled Hubbard chain with open boundary conditions, Eq. (1). The rationale for choosing open boundary conditions is that this will make the following analysis simpler.

It is known from the exact solution that the energy eigenvalues of the open half-filled Hubbard model are equal to those of a tight-binding model of spinless fermions and that the degeneracies in the spectrum are due to the spin degrees of freedom [4]. Following Ref. [80] we now construct a unitary transformation to spinless fermion and spin degrees of freedom, that simplifies in the $U \to \infty$ limit and reproduces these features. We first express the fermion creation and annihilation operators in terms of new spinless fermion operators a_j and Pauli matrices σ_j^α as

$$c_{j,\uparrow}^\dagger = [a_j^\dagger - (-1)^j a_j]\sigma_j^+,$$
$$c_{j,\downarrow}^\dagger = a_j^\dagger \frac{1-\sigma_j^z}{2} + (-1)^j a_j \frac{1+\sigma_j^z}{2}. \tag{8}$$

The correspondence between the original spinful fermions and the spin and spinless fermion degrees of freedom is [80]

$$|0\rangle_j = |-\rangle_j \otimes |\circ\rangle_j,\ |\uparrow\rangle_j = |+\rangle_j \otimes |\bullet\rangle_j,$$
$$|\downarrow\rangle_j = |-\rangle_j \otimes |\bullet\rangle_j,\ |\uparrow\downarrow\rangle_j = |+\rangle_j \otimes |\circ\rangle_j, \tag{9}$$

where $\sigma_j^z|\pm\rangle_j = \pm|\pm\rangle_j$ and $a_j|\circ\rangle_j = 0$, $|\bullet\rangle_j = a_j^\dagger|\circ\rangle_j$. In terms of the operators (8) the Hamiltonian reads $H = H_\infty + H_1$, where

$$H_\infty = -t\sum_{j=1}^{L-1} P_j[a_j^\dagger a_{j+1} + \text{H.c.}] + \frac{U}{2}\sum_{j=1}^{L}\left[\frac{1}{2} - a_j^\dagger a_j\right],$$
$$H_1 = -t\sum_{j=1}^{L-1}(-1)^j[a_j^\dagger a_{j+1}^\dagger + \text{H.c.}]\frac{\boldsymbol{\sigma}_j\cdot\boldsymbol{\sigma}_{j+1}-1}{2}. \tag{10}$$

Here we have defined

$$P_j = \frac{1+\vec{\sigma}_j\cdot\vec{\sigma}_{j+1}}{2}. \tag{11}$$

The pairing term H_1 changes the number of doubly occupied sites, which incurs a very large energy cost for $U \gg t$. As we are interested in the infinite-U limit we carry out a Schrieffer-Wolf transformation to remove the pairing term in (10):

$$e^{iS}He^{-iS} = H_\infty + O\left(\frac{t^2}{U}\right). \tag{12}$$

Here the generator S is taken in the form of a t/U expansion [81]

$$S = \sum_{n=1}\left(\frac{t}{U}\right)^n S^{(n)}. \tag{13}$$

In order to obtain (12) we choose the leading term to be

$$S^{(1)} = -i\sum_{j=1}^{L-1}(-1)^j[a_j^\dagger a_{j+1}^\dagger - \text{H.c.}]\frac{\boldsymbol{\sigma}_j\cdot\boldsymbol{\sigma}_{j+1}-1}{2}. \tag{14}$$

The main utility of the representation (12) is that the spin degrees of freedom can now be removed from the Hamiltonian by a unitary transformation [80]

$$\mathcal{U} = \prod_{\ell=1}^{L-1}[(1-n_{\ell+1}) + n_{\ell+1}P_\ell P_{\ell-1}\ldots P_1]. \tag{15}$$

This step makes use of the open boundary conditions and is more involved in the periodic case. One has

$$\tilde{H}_\infty = \mathcal{U}^\dagger H_\infty \mathcal{U}$$
$$= -t\sum_{j=1}^{L-1}[a_j^\dagger a_{j+1} + \text{H.c.}] - \frac{U}{2}\left[\hat{N} - \frac{L}{2}\right], \tag{16}$$

where $\hat{N} = \sum_{j=1}^{L} a_j^\dagger a_j$. The Hamiltonian (16) is straightforwardly diagonalized by going to Fourier space

$$a(k_n) = \sqrt{\frac{2}{L+1}} \sum_{j=1}^{L} \sin(k_n j)\, a_j, \tag{17}$$

where

$$k_n = \frac{\pi n}{L+1}, \quad n = 1, \ldots, L. \tag{18}$$

In terms of the Fourier modes the Hamiltonian is diagonal:

$$\tilde{H}_\infty = \sum_{k_n} \epsilon(k_n) a^\dagger(k_n) a(k_n) + \frac{UL}{4}, \tag{19}$$

where the single-particle dispersion is

$$\epsilon(p) = -\frac{U}{2} - 2t\cos(p). \tag{20}$$

This shows, in accordance with the exact solution [4], that in the infinite-U limit the dynamics of the half-filled open Hubbard model is determined by the noninteracting spinless fermion Hamiltonian (16). For future reference we note that the ground state of (16) corresponds to a completely filled band:

$$|\mathrm{GS}\rangle = \prod_{j=1}^{L} a_j^\dagger |0\rangle. \tag{21}$$

We now want to use the strong-coupling formalism developed above to determine dynamical correlation functions at finite temperatures. For simplicity we begin by considering the density-density correlator.

A. Density correlations at finite temperature

We can use the above setup for determining density correlations in a particular parameter regime of the half-filled Hubbard model as follows. For strong interactions the Mott gap is proportional to the Hubbard interaction U, while the characteristic energy scale in the spin sector of the theory is t^2/U. The "charge-sector only" theory then applies (as the leading approximation in t/U) in the window

$$\frac{t^2}{U} \ll T, \omega, t. \tag{22}$$

At $T = 0$ the density-density response function vanishes for frequencies below twice the Mott gap, but at $T > 0$ a nonzero response develops and can be determined in the framework of the model (16). As the density of double-occupied sites is very small in the regime (22), we may apply the low-density approach of Refs. [78,79,82,83] to finite-temperature dynamical correlation functions. The correlator of interest is

$$C_{\ell,m}(t) = \frac{1}{Z}\mathrm{Tr}\{e^{-\beta H}[\rho_\ell(t), \rho_m(0)]\}, \tag{23}$$

where

$$\rho_j = \sum_{\sigma=\uparrow,\downarrow} c_{j,\sigma}^\dagger c_{j,\sigma} = 1 + \sigma_j^z (1 - a_j^\dagger a_j). \tag{24}$$

In the transformed basis we have

$$\begin{aligned}\tilde{\rho}_\ell &= \mathcal{U}^\dagger \rho_\ell \mathcal{U} + O(t/U) \\ &= 1 + (1 - n_\ell) \sum_{j=0}^{L-\ell} \sigma_{L-j}^z \, P_j^{(\ell+1)} + O(t/U),\end{aligned} \tag{25}$$

where $P_k^{(\ell+1)}$ projects onto states with k unoccupied sites (in the spinless fermion variables) in the interval $[\ell+1, L]$

$$P_k^{(\ell+1)} = \sum_{\ell < p_1 < \cdots < p_k \leqslant L} \prod_{j=1}^{k} (1 - n_{p_j}) \prod_{\substack{l=\ell+1 \\ l \neq p_s}}^{L} n_l. \tag{26}$$

Here we have defined $P_0^{(L+1)} = 1$. The leading contribution to (23) in the framework of a t/U expansion is given by

$$C_{\ell,m}(t) \simeq \frac{1}{Z}\mathrm{Tr}\{e^{-\beta \tilde{H}_\infty}[\tilde{\rho}_\ell(t), \tilde{\rho}_m(0)]\}, \tag{27}$$

where

$$\tilde{\rho}_\ell(t) = e^{i\tilde{H}_\infty t} \tilde{\rho}_\ell e^{-i\tilde{H}_\infty t}. \tag{28}$$

We note that at zero temperature the dynamical correlator (27) is of order $O(t^2/U^2)$; see, e.g., Ref. [13]. This is beyond the accuracy in t/U we are working in here. The trace in (27) is over both charge and spin degrees of freedom. As these are uncoupled in the leading order in the t/U expansion we have

$$\frac{1}{Z}\mathrm{Tr}(e^{-\beta \tilde{H}_\infty} \mathcal{O}_c \mathcal{O}_s) = \frac{\mathrm{Tr}_c(e^{-\beta \tilde{H}_\infty} \mathcal{O}_c)}{Z_c} \frac{\mathrm{Tr}_s(\mathcal{O}_s)}{2^L}, \tag{29}$$

where $\mathcal{O}_{c,s}$ are any operators that act nontrivially only on the charge and spin degrees of freedom, respectively. As the spin degrees of freedom do not have any dynamics at leading order in the t/U expansion we have

$$\sigma_\ell^z(t) = \sigma_\ell^z, \quad 2^{-L}\mathrm{Tr}_s\left(\sigma_\ell^z \sigma_n^z\right) = \delta_{\ell,n}. \tag{30}$$

This allows us to reduce the calculation of (27) to the charge sector only:

$$C_{\ell,m}(t) \simeq \sum_{j=0}^{L-\min(\ell,m)} \frac{1}{Z_c}\mathrm{Tr}_c\{e^{-\beta \tilde{H}_\infty}[\mathcal{A}_{\ell,j}(t), \mathcal{A}_{m,j}]\}, \tag{31}$$

where

$$\mathcal{A}_{\ell,j}(t) = [1 - n_\ell(t)] P_j^{(\ell+1)}(t). \tag{32}$$

As the charge sector is a free theory (31) can now in principle be calculated using Wick's theorem and a determinant representation can be obtained. As this is somewhat involved we focus on low temperatures and proceed by applying the formalism of Refs. [78,79,82,83], which is possible as in the window (22) the density of thermally excited spinless fermions is small. To proceed, we express (31) in a Lehmann representation and then cast it in the form of a linked cluster expansion. The leading contribution in our window (22) is

$$C_{\ell,n}(t) \simeq \sum_p e^{\beta\epsilon(p)} \langle p|[\mathcal{A}_{\ell,0}(t), \mathcal{A}_{n,0}]|p\rangle + O(e^{-\beta U}). \tag{33}$$

Here $|p\rangle$ is a one-hole state

$$|p\rangle = \sqrt{\frac{2}{L+1}} \sum_j \sin(pj) a_j |\mathrm{GS}\rangle, \tag{34}$$

with energy $-\epsilon(p)$ relative to the ground state, and the momenta are quantized according to (18). We note that one-hole states have to be taken into account as we are working in the grand canonical ensemble, where the total number of spinless fermions is not fixed. Evaluating the expectation value in (33) gives

$$C_{\ell,n}(t) \simeq \frac{4i}{L+1}\mathrm{Im}\sum_{p} e^{(\beta-it)\epsilon(p)}\sin(p\ell)\sin(pn) \times G(\ell,n,t), \tag{35}$$

where $G(\ell,n,t)$ is the zero-temperature Green's function of our spinless fermions:

$$G(\ell,n,t) = \frac{2}{L+1}\sum_{k}\sin(k\ell)\sin(kn)e^{i\epsilon(k)t}. \tag{36}$$

We now focus on ℓ,n in the middle of our open chain, where the correlation functions are translationally invariant for sufficiently large system sizes, so that $C_{\ell,n}(t) \to \mathcal{C}(\ell-n,t)$. Taking the $L\to\infty$ limit we have

$$\mathcal{C}(m,t) = 2i\mathrm{Im}\int_{-\pi}^{\pi}\frac{dk\,dp}{(2\pi)^2}e^{\beta\epsilon(p)+i(p+k)m+it[\epsilon(k)-\epsilon(p)]}. \tag{37}$$

We are interested in the real part of the Fourier transform of $\mathcal{C}(m,t)$:

$$\chi(\omega,Q) = \mathrm{Re}\left[\int_0^\infty dt\sum_{m=-\infty}^{\infty}e^{i\omega t-iQm}\,\mathcal{C}(m,t)\right] \simeq \frac{1-e^{-\beta\omega}}{2}\theta(|4t\sin(Q/2)|-|\omega|) \times \frac{e^{\beta\epsilon(P+Q/2)}+e^{\beta\epsilon(P-Q/2-\pi)}}{\sqrt{[4t\sin(Q/2)]^2-\omega^2}}, \tag{38}$$

where $\theta(x)$ is the Heaviside function and P is given by

$$P = \arcsin\left(\frac{\omega}{4t\sin(Q/2)}\right). \tag{39}$$

We see that in the window (22) a finite-temperature resonance develops as the temperature is increased, which follows the "dispersion"

$$\omega_Q = 4t|\sin(Q/2)|. \tag{40}$$

This is very reminiscent of the Villain mode in the spin-1/2 Heisenberg chain [77,78]. We note that the square root singularity in (38) is an artifact of the low-density expansion and will be smoothed by higher order contributions [78,79]. In Fig. 6 we plot $\chi(\omega,Q)$ for $U/t=20$ and $\beta t=2$. The results of the strong-coupling expansion can be compared to those obtained by tDMRG; cf. Fig. 5. As the numerical simulations were carried out at intermediate interaction strengths $U=8t$ only a qualitative comparison is possible. The dominant feature in the charge dynamical structure factor at $U=8t$ occurs at frequencies above approximately twice the $T=0$ Mott gap. This feature evolves smoothly with temperature and as we have remarked before corresponds to the $O(t^2/U^2)$ contribution in the strong-coupling expansion. This is beyond the accuracy of the analytical calculation presented above. At low frequencies within the $T=0$ Mott gap the charge dynamical structure factor shown in Fig. 5 displays a weak feature that is qualitatively quite similar to the Villain-like mode obtained in the framework of the strong-coupling expansion; cf. Fig. 6.

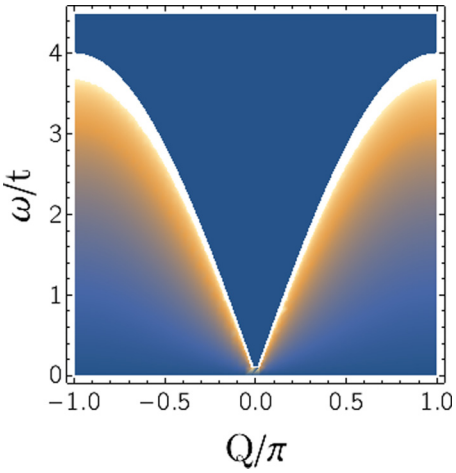

FIG. 6. Density-density correlator at low frequencies for $U/t=20$ and $\beta t=2$. The spectral weight increases with temperature in our window (22) and is concentrated around the "dispersion" (40).

B. Single-particle spectral function

We now turn to the single-particle Green's function:

$$\mathcal{G}(m,\ell,t) = \frac{1}{Z}\mathrm{Tr}[e^{-\beta H_\infty}\{c_{m,\uparrow},c^\dagger_{\ell,\uparrow}(t)\}]. \tag{41}$$

At leading order in t/U this becomes

$$\mathcal{G}(m,\ell,t) \simeq \frac{1}{Z_cZ_s}\mathrm{Tr}[e^{-\beta\tilde{H}_\infty}\{\tilde{c}_{m,\uparrow},\tilde{c}^\dagger_{\ell,\uparrow}(t)\}], \tag{42}$$

where

$$\tilde{c}_{m,\uparrow} = \mathcal{U}^\dagger c_{m,\uparrow}\mathcal{U}. \tag{43}$$

A complication compared to the case of the density operator considered above is that the fermion operators are very complicated in the transformed basis. However, it is possible to isolate the terms required for the purposes of a low-temperature expansion. We find for $1<\ell<L$

$$\tilde{c}^\dagger_{\ell,\uparrow} = a^\dagger_\ell\prod_{j=\ell+1}^{L}n_j\sigma^+_{L-\ell+1}\mathcal{S}^\dagger_{L-\ell+1,L} - (-1)^\ell a_\ell\prod_{j=\ell+1}^{L}n_j\,\mathcal{S}_{L-\ell+1,L}\,\sigma^+_{L-\ell+1}+\cdots, \tag{44}$$

where we have defined

$$\mathcal{S}_{n,L}|\sigma_1,\ldots,\sigma_L\rangle = |\sigma_1,\ldots,\sigma_{n-1},\sigma_{n+1},\ldots,\sigma_L,\sigma_n\rangle. \tag{45}$$

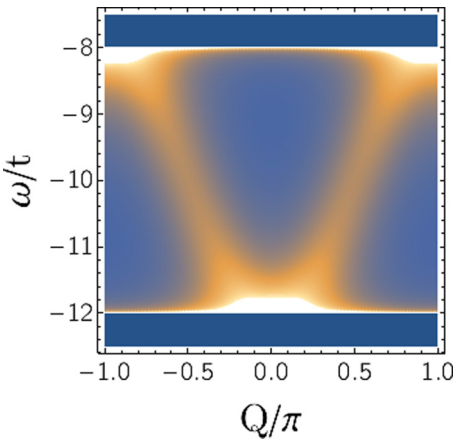

FIG. 7. Hole part of the spectral function at $U = 20t$.

The leading term in the low-temperature expansion of the single-particle Green's function is then

$$\mathcal{G}(m,\ell,t) \approx (-1)^{\ell-m}[G(\ell,m,t) + G(m,\ell,-t)] \times \frac{\mathrm{Tr}_s[\sigma^-_{L-m+1}\mathcal{S}^\dagger_{L-m+1,L}\mathcal{S}_{L-\ell+1,L}\sigma^+_{L-\ell+1}]}{2^L} = \frac{(-1)^{\ell-m}[G(\ell,m,t) + G(m,\ell,-t)]}{2^{|\ell-m|+1}}, \quad (46)$$

where $G(m,\ell,t)$ is given by (36). Focusing again on the center of the chain where the Green's function is translationally invariant, Fourier transforming, and then taking the real part, we obtain the single-particle spectral function:

$$A(\omega,Q) \approx \frac{3\theta(2t - |\omega + U/2|)}{8t|\sin(k_0)|}\left[\frac{1}{5 + 4\cos(Q - k_0)} + \frac{1}{5 + 4\cos(Q + k_0)}\right] + \{\omega \to -\omega\},$$
$$k_0 = \arccos\left(-\frac{\omega + U/2}{2t}\right). \quad (47)$$

The expression (47) has threshold singularities at

$$|\omega \pm U/2| = 2t. \quad (48)$$

These are an artifact of working at lowest order in the low-density expansion and a summation of higher order contributions will smooth out these singularities. In Fig. 7 we plot $A(\omega,Q)$ for $U/t = 20$.

The results of the strong-coupling low-temperature expansion can again be compared qualitatively to those obtained by tDMRG. The hole part of the spectral function for $U = 8t$, $T = t$ shown in Fig. 4(c) looks very similar to the result displayed in Fig. 7. The main differences are due to the finite bandwidth of the spin degrees of freedom at $U = 8t$, which leads to a bending of the straight-line features at $\omega = -U/2 \pm 2t$ in the strong-coupling expansion. The general "$\overline{\mathrm{V}}$-shaped" structure of the response and the concentration of spectral weight around the points $\omega = -U/2 - 2t$, $Q = 0$ and $\omega = -U/2 + 2t$, $Q = \pm\pi$ is already clearly visible in the $U = 8t$ data.

V. CONCLUSIONS

We have investigated the finite-temperature behavior of the photoemission spectrum of one-dimensional Mott insulators with spin-charge separation. We considered the one-dimensional half-filled Hubbard chain and determined dynamical response functions by a combination of finite-temperature tDMRG methods and an analytic strong-coupling approach in the spin-incoherent regime. The single-particle spectral function displays an interesting evolution with temperature. The spinon and holon branches in the photoemission spectrum evolve into a broad dispersive band, while at higher frequencies a second broad band of excitation emerges. At elevated temperatures these features can be described in terms of a picture reminiscent of the Hubbard-I approximation, where spin correlations are completely washed out. Interestingly, unlike the two-dimensional counterpart, in one-dimension the hopping amplitude (effective mass) is not renormalized. In the window $4t^2/U \ll T \ll U$ a spin-incoherent regime emerges. This can be described by an analytic strong-coupling expansion. The single-particle spectral function in this regime displays a characteristic "$\overline{\mathrm{V}}$-shaped" structure.

In the density-density correlation function the "melting" of the Mott gap is accompanied by the emergence of a temperature-induced resonance at low frequencies. This feature can be understood in terms of transitions between thermally occupied levels and is akin to the celebrated Villain mode in gapped antiferromagnets.

ACKNOWLEDGMENTS

We thank R. Hulet and B. Bertini for illuminating discussions. This work was supported by the US Department of Energy, Office of Basic Energy Sciences (A.E.F.) and Materials Sciences and Engineering Division (A.N.), under Grant No. DE-SC0014407 (A.E.F.), and by the EPSRC under Grant No. EP/N01930X/1 (F.H.L.E.).

[1] F. D. M. Haldane, J. Phys. C **14**, 2585 (1981).
[2] A. O. Gogolin, A. A. Nerseyan, and A. M. Tsvelik, *Bosonization and Strongly Correlated Systems* (Cambridge University Press, Cambridge, 1998).
[3] T. Giamarchi, *Quantum Physics in One Dimension* (Clarendon Press, Oxford, 2004).
[4] F. Essler, H. Frahm, F. Göhmann, A. Klümper, and V. E. Korepin, *The One-Dimensional Hubbard Model* (Cambridge University Press, Cambridge, 2010).
[5] H. Frahm and V. E. Korepin, Phys. Rev. B **42**, 10553 (1990).
[6] H. Eskes, M. B. J. Meinders, and G. A. Sawatzky, Phys. Rev. Lett. **67**, 1035 (1991).
[7] P. Phillips, Rev. Mod. Phys. **82**, 1719 (2010).
[8] A. Damascelli, Z. Hussain, and Z.-X. Shen, Rev. Mod. Phys. **75**, 473 (2003).
[9] J. Meng, G. Liu, W. Zhang, L. Zhao, H. Liu, X. Jia, D. Mu, S. Liu, X. Dong, J. Zhang *et al.*, Nature (London) **462**, 335 (2009).
[10] S. Sorella and A. Parola, J. Phys.: Condens. Matter **4**, 3589 (1991).
[11] T. Xiang and N. d'Ambrumenil, Phys. Rev. B **45**, 8150 (1992).

[12] K. Penc and M. Serhan, Phys. Rev. B **56**, 6555 (1997).
[13] K. Penc, K. Hallberg, F. Mila, and H. Shiba, Phys. Rev. B **55**, 15475 (1997).
[14] E. Jeckelmann, F. Gebhard, and F. H. L. Essler, Phys. Rev. Lett. **85**, 3910 (2000).
[15] H. Benthien, F. Gebhard, and E. Jeckelmann, Phys. Rev. Lett. **92**, 256401 (2004).
[16] J. M. P. Carmelo, K. Penc, L. M. Martelo, P. D. Sacramento, J. M. B. L. Dos Santos, R. Claessen, M. Sing, and U. Schwingenschlögl, Europhys. Lett. **67**, 233 (2004).
[17] J. M. P. Carmelo, K. Penc, P. D. Sacramento, M. Sing, and Claessen, J. Phys.: Condens. Matter **18**, 5191 (2006).
[18] J. M. P. Carmelo, D. Bozi, and K. Penc, J. Phys.: Condens. Matter **20**, 415103 (2008).
[19] M. Kohno, Phys. Rev. Lett. **105**, 106402 (2010).
[20] T. L. Schmidt, A. Imambekov, and L. I. Glazman, Phys. Rev. Lett. **104**, 116403 (2010).
[21] R. G. Pereira and E. Sela, Phys. Rev. B **82**, 115324 (2010).
[22] F. H. L. Essler, Phys. Rev. B **81**, 205120 (2010).
[23] T. L. Schmidt, A. Imambekov, and L. I. Glazman, Phys. Rev. B **82**, 245104 (2010).
[24] A. Imambekov, T. L. Schmidt, and L. I. Glazman, Rev. Mod. Phys. **84**, 1253 (2012).
[25] L. Seabra, F. H. L. Essler, F. Pollmann, I. Schneider, and T. Veness, Phys. Rev. B **90**, 245127 (2014).
[26] F. H. L. Essler, R. G. Pereira, and I. Schneider, Phys. Rev. B **91**, 245150 (2015).
[27] A. C. Tiegel, T. Veness, P. E. Dargel, A. Honecker, T. Pruschke, I. P. McCulloch, and F. H. L. Essler, Phys. Rev. B **93**, 125108 (2016).
[28] T. Veness and F. H. L. Essler, Phys. Rev. B **93**, 205101 (2016).
[29] C. Yang and A. E. Feiguin, Phys. Rev. B **93**, 081107 (2016).
[30] J. Voit, Eur. Phys. J. B **5**, 505 (1998).
[31] B. Doyon and S. Lukyanov, Nucl. Phys. B **644**, 451 (2002).
[32] V. Lante and A. Parola, Phys. Rev. B **80**, 195113 (2009).
[33] R. G. Pereira, K. Penc, S. R. White, P. D. Sacramento, and J. M. P. Carmelo, Phys. Rev. B **85**, 165132 (2012).
[34] B. Schoenauer, P. Schmitteckert, and D. Schuricht, Phys. Rev. B **95**, 205103 (2017).
[35] A. Abendschein and F. F. Assaad, Phys. Rev. B **73**, 165119 (2006).
[36] A. E. Feiguin and G. A. Fiete, Phys. Rev. Lett. **106**, 146401 (2011).
[37] H. Matsueda, N. Bulut, T. Tohyama, and S. Maekawa, Phys. Rev. B **72**, 075136 (2005).
[38] F. H. L. Essler and A. M. Tsvelik, Phys. Rev. Lett. **90**, 126401 (2003).
[39] A. Mielke, J. Stat. Phys. **62**, 509 (1991).
[40] K. A. Matveev, Phys. Rev. Lett. **92**, 106801 (2004).
[41] G. A. Fiete and L. Balents, Phys. Rev. Lett. **93**, 226401 (2004).
[42] V. V. Cheianov and M. B. Zvonarev, Phys. Rev. Lett. **92**, 176401 (2004).
[43] V. V. Cheianov, H. Smith, and M. B. Zvonarev, Phys. Rev. A **71**, 033610 (2005).
[44] G. A. Fiete, Rev. Mod. Phys. **79**, 801 (2007).
[45] B. I. Halperin, J. Appl. Phys. **101**, 081601 (2007).
[46] A. E. Feiguin and G. A. Fiete, Phys. Rev. B **81**, 075108 (2010).
[47] M. Soltanieh-ha and A. E. Feiguin, Phys. Rev. B **90**, 165145 (2014).
[48] C. Kim, A. Y. Matsuura, Z.-X. Shen, N. Motoyama, H. Eisaki, S. Uchida, T. Tohyama, and S. Maekawa, Phys. Rev. Lett. **77**, 4054 (1996).
[49] C. Kim, Z.-X. Shen, N. Motoyama, H. Eisaki, S. Uchida, T. Tohyama, and S. Maekawa, Phys. Rev. B **56**, 15589 (1997).
[50] B. J. Kim, H. Koh, E. Rotenberg, S.-J. Oh, H. Eisaki, N. Motoyama, S. Uchida, T. Tohyama, S. Maekawa, Z.-X. Shen, and C. Kim, Nat. Phys. **2**, 397 (2006).
[51] T. E. Kidd, T. Valla, P. D. Johnson, K. W. Kim, G. D. Gu, and C. C. Homes, Phys. Rev. B **77**, 054503 (2008).
[52] K. Kobayashi, T. Mizokawa, A. Fujimori, M. Isobe, Y. Ueda, T. Tohyama, and S. Maekawa, Phys. Rev. Lett. **82**, 803 (1999).
[53] Y. Sagi, T. E. Drake, R. Paudel, R. Chapurin, and D. S. Jin, Phys. Rev. Lett. **114**, 075301 (2015).
[54] I. G. White, R. G. Hulet, and K. R. A. Hazzard, arXiv:1612.05671.
[55] S. R. White and A. E. Feiguin, Phys. Rev. Lett. **93**, 076401 (2004).
[56] A. J. Daley, C. Kollath, U. Schollwöck, and G. Vidal, J. Stat. Mech. (2004) P04005.
[57] A. E. Feiguin, AIP Conf. Proc. **1419**, 5 (2011).
[58] A. E. Feiguin, in *Strongly Correlated Systems*, edited by A. Avella and F. Mancini, Springer Series in Solid-State Sciences Vol. 176 (Springer, Berlin, Heidelberg, 2013).
[59] A. E. Feiguin and S. R. White, Phys. Rev. B **72**, 220401 (2005).
[60] Y. Takahashi and H. Umezawa, Collect. Phenom. **2**, 55 (1975).
[61] H. Umezawa, H. Matsumoto, and M. Tachiki, *Thermo-Field Dynamics and Condensed States* (North-Holland, Amsterdam, 1982).
[62] H. Matsumoto, in *Progress in Quantum Field Theory* (North-Holland, Amsterdam, 1986), p. 171.
[63] M. Suzuki, J. Phys. Soc. Jpn. **12**, 4483 (1985).
[64] M. Suzuki, J. Stat. Phys. **42**, 1047 (1985).
[65] S. M. Barnett and P. L. Knight, Phys. Rev. A **38**, 1657 (1988).
[66] S. M. Barnett and P. L. Knight, J. Opt. Soc. Am. B **2**, 467 (1985).
[67] A. Nocera and G. Alvarez, Phys. Rev. B **93**, 045137 (2016).
[68] T. Barthel, Phys. Rev. B **94**, 115157 (2016).
[69] C. Karrasch, J. H. Bardarson, and J. E. Moore, New J. Phys. **15**, 083031 (2013).
[70] M. Ogata and H. Shiba, Phys. Rev. B **41**, 2326 (1990).
[71] M. Ogata, T. Sugiyama, and H. Shiba, Phys. Rev. B **43**, 8401 (1991).
[72] H. Suzuura and N. Nagaosa, Phys. Rev. B **56**, 3548 (1997).
[73] M. Brunner, F. F. Assaad, and A. Muramatsu, Eur. Phys. J. B **16**, 209 (2000).
[74] M. Kohno, Phys. Rev. Lett. **108**, 076401 (2012).
[75] A. Dorneich, M. G. Zacher, C. Gröber, and R. Eder, Phys. Rev. B **61**, 12816 (2000).
[76] C. Gröber, R. Eder, and W. Hanke, Phys. Rev. B **62**, 4336 (2000).
[77] J. Villain, Phys. B+C **79**, 1 (1975).
[78] A. J. A. James, W. D. Goetze, and F. H. L. Essler, Phys. Rev. B **79**, 214408 (2009).
[79] W. D. Goetze, U. Karahasanovic, and F. H. L. Essler, Phys. Rev. B **82**, 104417 (2010).
[80] B. Kumar, Phys. Rev. B **79**, 155121 (2009).
[81] A. H. MacDonald, S. M. Girvin, and D. Yoshioka, Phys. Rev. B **37**, 9753 (1988).
[82] A. J. A. James, F. H. L. Essler, and R. M. Konik, Phys. Rev. B **78**, 094411 (2008).
[83] F. H. L. Essler and R. M. Konik, J. Stat. Mech. (2009) P09018.